Soft Matter

PAPER

View Article Online
View Journal | View Issue

Cite this: *Soft Matter*, 2022, **18**, 6800

Experimental investigation and finite element modelling of PMMA/carbon nanotube nanobiocomposites for bone cement applications

Vahideh Sadati,[a] Mehrdad Khakbiz,*[a] Milad Chagami,[a] Reza Bagheri,[b] Fatemeh Salahi Chashmi,[b] Babak Akbari,[a] Sara Shakibania[a] and Ki-Bum Lee[c]

Multi-walled carbon nanotubes (MWCNTs) are one of the preferred candidates for reinforcing polymeric nanobiocomposites, such as acrylic bone type of cement. In this study, at first, bulk samples of the reinforced polymethylmethacrylate (PMMA) matrix were prepared with 0.1, 0.25, and 0.5 wt per wt% of MWCNTs by the casting method. Tensile and three-point bending tests were performed to determine the essential mechanical properties of bone cement, such as tensile and bending strengths. The tensile fracture surfaces were investigated by scanning electron microscopy (SEM). The commercial software (Abaqus) was used to conduct finite element analysis (FEA) by constructing a representative volume element (RVE) model for numerically computing the tensile and bending parameters of PMMA-MWCNT nanocomposites. Finally, MTT assays were utilized to evaluate the cell viability on the surface of nanobiocomposites. The results show that by increasing the MWCNT amount in the PMMA-based cement, the bending strengths (BS), tensile strength (TS), and elastic modulus (EM) increased considerably. Furthermore, the disparity between the FEA and experimental TS, EM, and BS values was less than 20%. According to MTT viability experiments, adding MWCNTs to PMMA had no influence on PMMA toxicity and resulted in a negative response to interaction with mesenchymal stem cells. The cell density on the nanobiocomposite was more than pristine-PMMA.

Received 16th May 2022,
Accepted 28th July 2022

DOI: 10.1039/d2sm00637e

rsc.li/soft-matter-journal

1 Introduction

Multi-walled carbon nanotubes (MWCNTs) exhibit many desirable properties, including flexibility, high strength, resistance to transverse and torsional displacements, and the ability to be pulled without breaking. Theoretical studies have shown that MWCNTs are one of the hardest materials ever synthesized at the time of their discovery and experimental study.[1] For example, the elastic modulus for single-walled carbon nanotubes (SWCNTs) is nearly 1 TPa, and for MWCNTs it is in the range of 1–3 TPa. These excellent mechanical, thermal, and electrical properties of CNTs make them attractive solid nanofiber reinforcements in composite materials.[2–4]

One of the most prominent orthopedic applications of polymers is using them as a matrix for bone cement composites. In this regard, degradable polymers are used as fillers in the damaged areas of the bone or for fixation of the prosthesis around the bone-tissues. Through the bone regeneration process, the polymeric cement is chemically degraded by a hostile *in vivo* environment. These materials mainly consist of two phases: solid phase (including polymethylmethacrylate, copolymer, methylmethacrylate-styrene, barium sulfate, and benzoyl peroxide (BPO)), and liquid (including methyl methacrylate, anhydrous methyl pyrrolidine, and hydroquinone), and by mixing them, a hard polymer is obtained. Dibenzoyl peroxide is used as a reaction initiator, whereas dimethyl toluidine and hydroquinone are used as reaction activators and inhibitors, respectively. Barium sulfate acts as an X-ray absorbent in the bone cement composition, resulting in more contrast in the radiographic image. The presence of methyl methacrylate in bone-cements increases mechanical properties and accelerates the cement to be networking.[5–7]

One problem of the various bone cement is their weak chemical and mechanical properties. An ideal bone cement must conform to the mechanical behavior of the bone-tissue and create a consistent interface with the surrounding tissues, be biocompatible, and should not provide an environment for the growth of microbes. Many studies have been conducted for investigation of nano biomaterials for biomedical application.[6,37] Because CNTs have excellent chemical and physical properties, the combination

[a] *Division of Biomedical Engineering, Faculty of New Sciences and Technologies, University of Tehran, North Kargar Ave., PO Box 14395-1561, Tehran, Iran. E-mail: Khakbiz@ut.ac.ir*
[b] *Department of Materials science and Engineering, Sharif University of Technology, Tehran, Iran*
[c] *Department of Chemistry and Chemical Biology Rutgers, The State University of New Jersey, Piscataway, NJ 08854, USA*

of PMMA and MWCNTs is very promising for biomedical applications.[7,8] Ormsby *et al.*[9] studied the properties of fatigue and biocompatibility of bone cement of the PMMA/MWCNT composite. In this research, the amounts of MWCNT in the composites have been 0.1–1 wt%. The results of this study showed that MWCNT increases fatigue life, and low percentages of MWCNT (0.1 wt%) have the best effect on improving properties. Also, the 63-MG bone cells were well bonded to the surface of all bone cement. Yu Hsun Nien *et al.*[10] also showed that the tensile and compression strength of the sample containing 0.1 wt% of CNTs was 18 wt%, 23 wt% higher than the monolithic polymer. In another study, Ormsby *et al.*[11] investigated the MWCNT/PMMA nanobiocomposite mechanical properties. As a result, they found that adding MWCNTs to PMMA up to 0.25 wt% improved the mechanical properties of the nanobiocomposite. Furthermore, 0.5 wt% led to less improvement in mechanical properties. Also, the dispersion of MWCNTs within the cement matrix is increased by adding chemical functional groups, with the carboxyl functionalized MWCNTs providing the most significant improvements in mechanical integrity. Numerous modeling studies have been carried out on composites containing CNTs using the finite element method.[16–20] Most research focus on a polymeric matrices such as epoxy,[18] nylon,[19] and polyurethane.[20] The most significant step in numerically evaluating the mechanical properties of PMMA-MWCNT nanocomposites is to develop a micromechanical model that allows for the microstructure effects on mechanical properties under load conditions to be investigated. For this purpose, Zhang *et al.*[21] used the digital imaging technique to produce finite element meshes. Wang *et al.*[22] and Peng *et al.*[23] produced microstructures based on the motion of particles from their regular positions, such as regular crystal networks. It is important to note that the representative volume element (RVE) size is an important parameter for making the micromechanical model. Gitman *et al.*[24] have discussed this in great detail. Therefore, the size of the RVE of any inhomogeneity, such as inclusion, void, and so on, should be smaller enough to estimate the micromechanical behavior of nanocomposites. The conclusion is that as the RVE size decreases, a more precise estimation will be performed.

Although several studies investigated the effects of MWCNTs on the mechanical properties of polymeric bone cement,[12–15] there is still no comprehensive experimental and numerical study on the effect of MWCNTs on the mechanical properties of the nanocomposite. Besides, the consideration of governing strengthening mechanisms is still in the infancy step.

In this study, the PMMA/MWCNT nanobiocomposites were initially manufactured using the casting process, and their mechanical properties were fully investigated. The effect of CNT amounts on tensile and bending properties, stiffness, and biocompatibility has been studied through experimental methods. In the second part, we evaluated the mechanical properties of these nano biocomposites using a simple RVE finite element model, and then evaluated the effect of process factors on these types of nanocomposites.

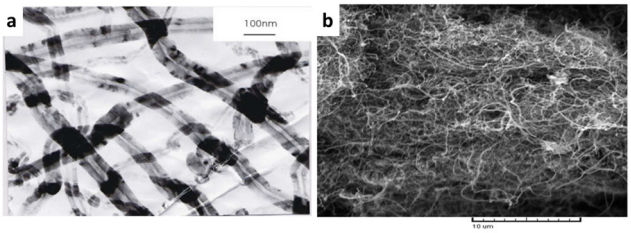

Fig. 1 The microstructure of multi-walled carbon nanotube represented by (a) TEM and (b) SEM images.

2 Materials and methods

2.1 Synthesis of PMMA-CNT nanocomposites

The acrylic brand Akro Pars was used as a polymeric matrix, purchased from the Marlik Medical Industries Company, Tehran, Iran. This product contains two powder and liquid components, and their compositions are shown in Table 1. MWCNTs were purchased from Tamad Kala Co. with an approximate average diameter of 40 nm were utilized as reinforcement (Fig. 1). Impurities such as cobalt and nickel were removed by immersion into the concentrated nitric acid (60 wt%) for 12 h. Then, they were rinsed with distilled water until pH 7 was achieved and then dried in an oven at 120 C.

The nanocomposites were synthesized using the following method: CNTs were mixed with a polymeric powder using a basic mixer. Then the liquid component was added (solid/liquid component ratio, 1 : 2), manually stirred, and cast in a flattened metal mold coated with Teflon. Due to the difference between the density of CNTs and powders, a uniform distribution was not achieved by employing this mixing method. The image of the sample produced is shown in Fig. 2a.

In the next step, the CNTs with the liquid component were mixed, and the powdered component was added to the mixture. Subsequently, it was stirred manually and then cast into the mold. The distribution of CNTs was improved in this method, but due to the high viscosity of the final mixture and the short curing time, the resulting mixture was non-uniform. Also, the reaction between two parts of the components did not occur, and transparent points in the sample are observable

Table 1 The number of different components used in the synthesis of the PMMA matrix

Liquid component		Solid powder component	%
Methyl methacrylate (monomer)	97.4 vol%	Poly methyl methacrylate	15 wt
N,*N*-Dimethyl-*p*-toluidine (dimethyl propiothetin)	2.6 vol%	Methyl methacrylate styrene copolymer	73.5 wt
Hydroquinone	75 ± 15 ppm	Di benzoyl peroxide	1.5 wt
		Barium sulfate	10 wt

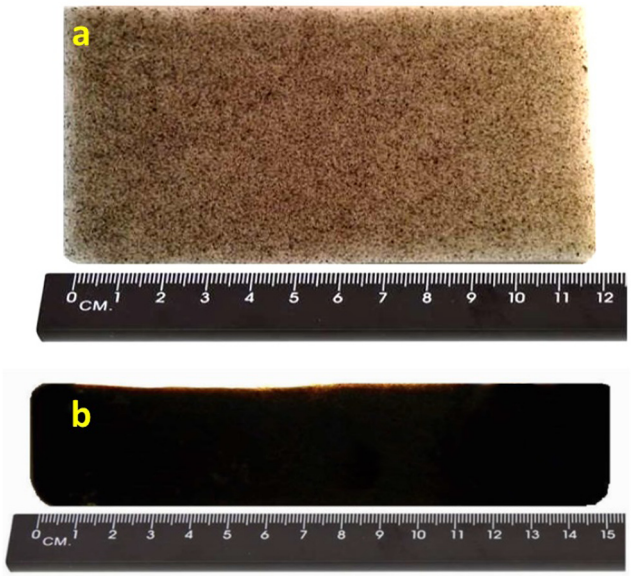

Fig. 2 The images of the PMMA bone cement samples (a) produced by simple mixing and (b) produced by ultrasonic mixing.

(see Fig. 2b). To solve this problem, we reduced the temperature of the mixture and the mold and increased the curing time. To extend the curing time, the initial 25% of the liquid was mixed with powder, and the remaining quantity (75%) was mixed with CNTs. Then the two components were mixed and poured into a mold. The weight ratio of the fabricated composites was determined as 0.1, 0.25, and 0.5 wt/wt% CNTs.

2.2 Mechanical properties

In this research, a tensile test was conducted to examine the mechanical properties of PMMA-based bone cement samples containing 0.1 wt%, 0.25 wt%, and 0.5 wt% MWCNTs. The experiment was performed according to the ASTM D638 standard at 5 min mm^{-1} speed and with three repetitions for each sample. Besides, the intact PMMA cast products were considered as the control specimens. A three-point bending test was employed to calculate the flexural strength of PMMA/MWCNT nanocomposites. According to ASTM D790, the test was conducted at a speed of 0.1 mm/min and under 10 N of a concentrated load.

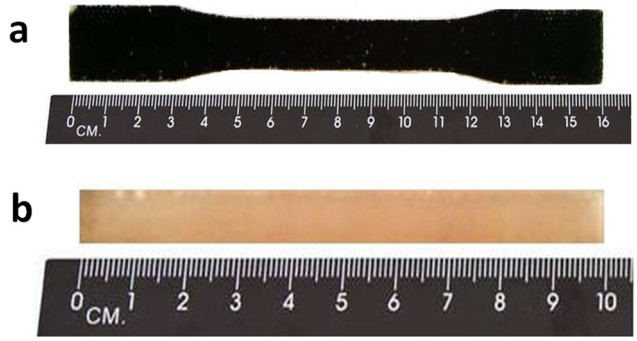

Fig. 3 The specimens used for the (a) tension, and (b) 3-point bending tests.

2.3 Morphological observation

Scanning electron microscopy (SEM) was used to investigate the fracture surfaces obtained from a uniaxial tensile test at the fracture point (Fig. 3).

2.4 MTT assay investigation

In this study, the MTT test was used to evaluate and compare the growth and proliferation of mesenchymal stem cells (rat bone marrow cells) on the surface of the samples. Test specimens were manufactured using polymer-based casting and the nanobiocomposites in a series of cylindrical plastic molds with a diameter of 15 and a height of 4 mm. The specimens were sterilized with alcohol and placed in the cell culture wells to perform the MTT test. 5000 cells were cultured on each sample, and the vessel was slowly transferred to the incubator. The culture medium contained Dulbecco's modified Eagle's medium (DMEM) and fetal bovine serum 10% (FBS). After 1, 3, 5, and 7 days, the growth medium was withdrawn from the samples, and 300 L of the solution (5 mg mL^{-1}) was added to each. The culture vessel was covered with an aluminum plate and placed in an incubator for 3 hours. Meanwhile, formazan crystals formed inside the cells. Then, dimethyl sulfoxide (DMSO) solvent was used to dissolve the crystals. The samples remained in the solvent for 10 minutes. At a wavelength of 570 nm, the cloudiness of the solution that was generated after the crystals were completely dissolved was measured. This test was repeated for each sample three times a day, and statistical

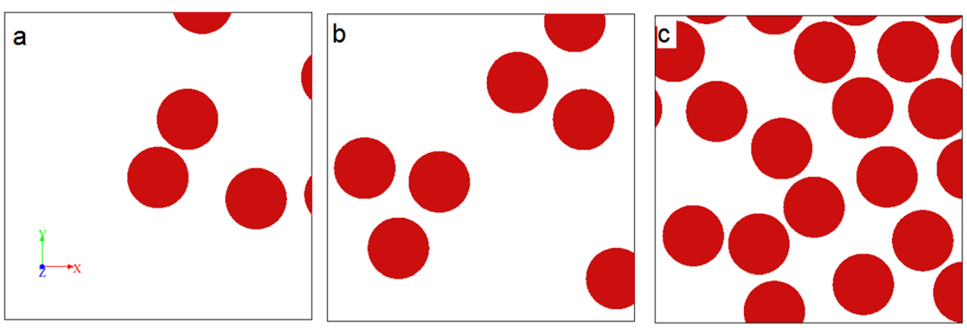

Fig. 4 Three two-dimensional geometries for (a) PMMA-CNTs 0.1 wt%, (b) PMMA-CNTs 0.25 wt% and (c) PMMA-CNTs 0.5 wt%.

analysis of the results was performed using PRISM software and ANOVA unilateral analysis.

2.5 Finite element modeling

In this research, in order to generate the appropriate micro-mechanical model by representing volume elements (RVE) the Digimat 2017.0 software was used. This model was developed by Liu Y. *et al.*[25] at first, and now it is used to simulate the properties of various nanocomposites. In this model, an RVE element is considered around the matrix/nanotubes, and it is obtained under constant strain across the CNTs and matrix. For the simulation process, a two-dimensional geometric shape of the composites was selected, while PMMA as a matrix and CNTs as the random inclusions. The direction of the CNTs was chosen to be parallel to the normal plane of the matrix, and the weight percent that was selected was 0.1, 0.25, and 0.5, respectively. The circular shape of CNTs was made in the Digimat-FE module. The algorithm proposed for dispersing the CNTs in the polymer matrix has been offered by Qing,[26] and it was also employed for this study. Then the model has transmitted to ABAQUS (ABAQUS-CAE 6.13) commercial software. Fig. 4 represents two-dimensional RVE shapes of the composites in which CNTs simply assumed as circle inclusions with a diameter of 40 nm. The finite element mesh models with quadrilateral elements were generated by the free technique meshing tool and a global approximately size of 2 nm (Fig. 5).

The mechanical properties of materials selected for modeling of the composite are shown in Table 2. Accordingly, the reinforcing phase is linearly elastic, and the polymer matrix was considered to exhibit elastoplastic behavior under the uniaxial tensile load. The definition of boundary condition is always necessary to solve a problem numerically. In this study, as it has been suggested by previous studies[26] periodic boundary condition was used for micromechanical models. Fig. 6 shows a schematic illustration of a periodic boundary condition in which all the nodes in node-sets have restricted to the nodes on opposite sides using the MPC subroutine. The nodes located in the corners at the bottom were considered to be free. The tensile stress was applied by the displacement of $Uz = 10$ from the top edge of models and by simulating a simple uniaxial tensile test.

Table 2 Mechanical properties of the composite model components

Material	Tensile strength (MPa)	Young modulus (MPa)	Poisson's ratio	Yield stress (MPa)
PMMA	33.6	2135	0.3	48.58
CNT	10 000	10 002	0.25	—

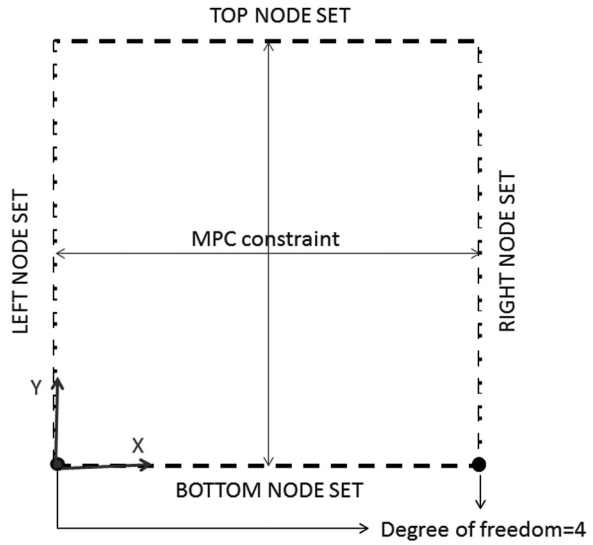

Fig. 6 Boundary condition in a schematic representation.

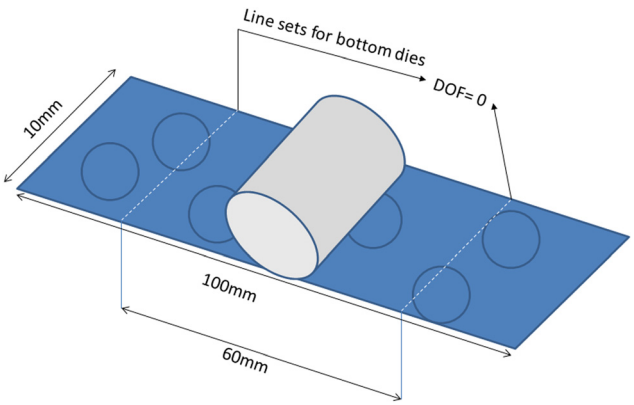

Fig. 7 Schematic illustration of the geometry used for modelling three-point bending of the PMMA-based bone cement nanocomposites.

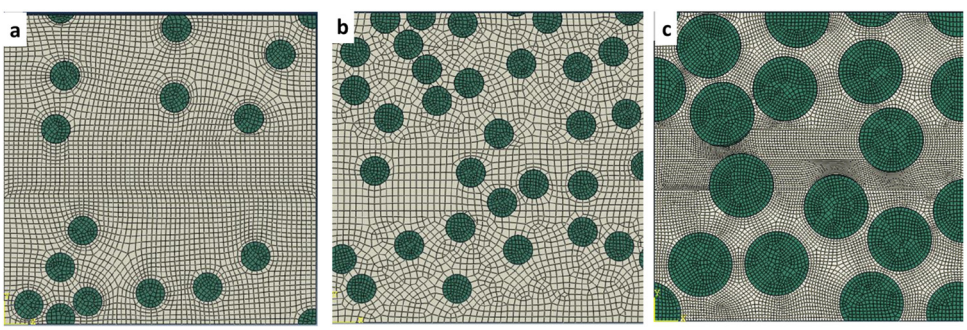

Fig. 5 Two-dimensional mesh models for uni-axial tensile test of (a) PMMA-CNTs 0.1 wt%, (b) PMMA-CNTs 0.2 wt% and (c) PMMA-CNTs 0.5 wt%.

Table 3 Experimental mechanical properties and FEA predictions for different samples

	Elongation (%)		EM (MPa)		TS (MPa)	
Specimen	Experimental	Numerical	Experimental	Numerical	Experimental	Numerical
PMMA	1.766 ± 0.138		2413 ± 14		24.5 ± 1.3	
PMMA/MWCNT(0.1)	1.560 ± 0.037	1.152 ± 0.23	2652 ± 26	2932 ± 27	30.6 ± 1.5	41.08 ± 1.5
PMMA/MWCNT(0.25)	1.257 ± 0.123	1.113 ± 0.19	2810 ± 29	3121 ± 31	35.9 ± 2.1	44.07 ± 1.8
PMMA/MWCNT(0.5)	1.212 ± 0.073	1.018 ± 0.07	3302 ± 6	3578 ± 41	36.7 ± 2.3	48.84 ± 2.6
PMMA/SMCNT(0.25)	1.123 ± 0.050		3369 ± 25		36.8 ± 1.7	

As is schematically shown in Fig. 7(a and b), the three-point bending test models with a symmetric boundary condition and centralized load-displacement were conducted to investigate the bending mechanical properties. Dimensions were determined according to ASTM D790. In addition, ABAQUS/standard coding and static load conditions for slow loading development were applied in each model. In the 2D models, two edge sets were utilized to be considered as the bearing die areas, and they were constrained in a way that the degree of freedom (DOF) of the line-sets be zero.

3 Results and discussion

3.1 Tensile mechanical properties

The average values of tensile strength, elastic modulus, and elongation percentage of intact PMMA (control sample) and the nanocomposites containing 0.1, 0.25, 0.5 wt% MWCNTs without surface modification and the sample with 0.25 wt% of surface-modified MWCNTs (SWCNTs) are presented in Table 3. Measurements indicate that the addition reinforcement phase to the matrix increases elastic modulus (EM) and tensile strength (TS) by up to 0.5 wt%. For example, by adding 0.5% MWCNTs, the tensile strength and elastic modulus increased by 50% and 37%, respectively. The obtained values can be approved effectively by those average amounts that have been reported by previous studies.[27,28] This enhancement is because the CNTs act as a load-bearing phase and show the shielding effect. It means that the applied load is transferred to the nanotubes instead of the polymer matrix. The strengthening effect of MWCNTs in PMMA bone cement shows the excellent adhesion between reinforcement and matrix and a homogeneous distribution of the nanotubes in bone cement. These

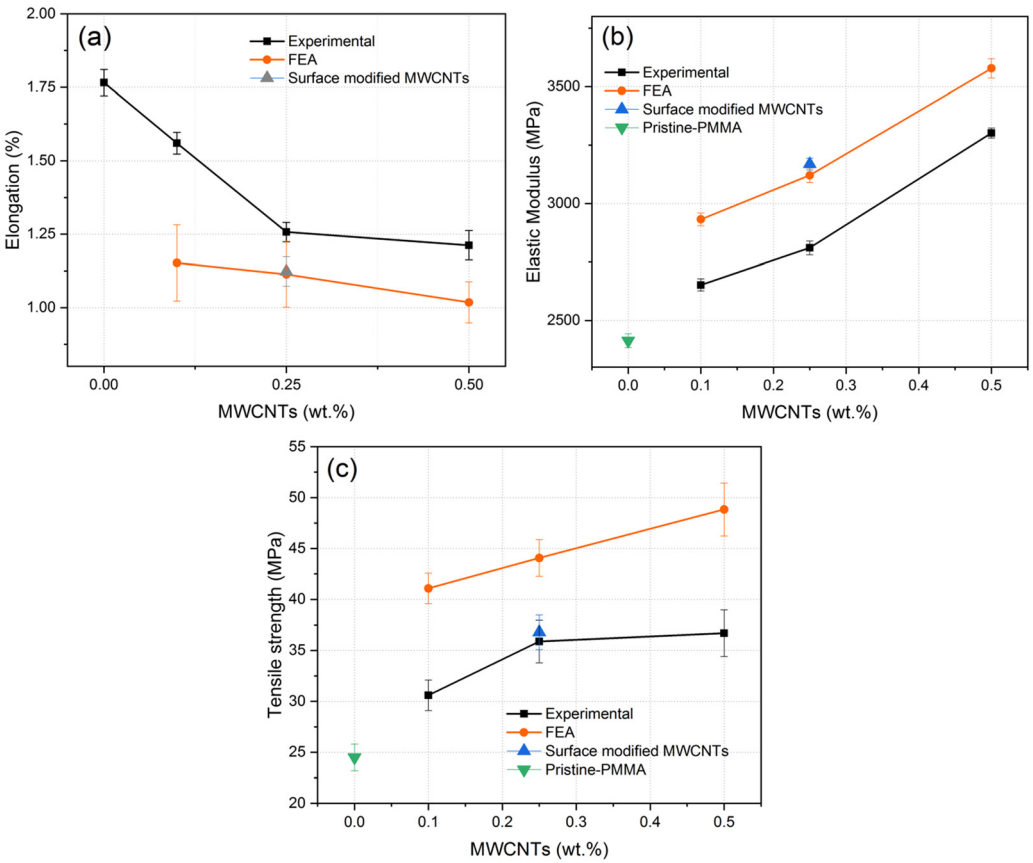

Fig. 8 Variation of experimental and FEA values of (a) % elongation, (b) EM, and (c) TS with the content of MWCNTs in the PMMA matrix.

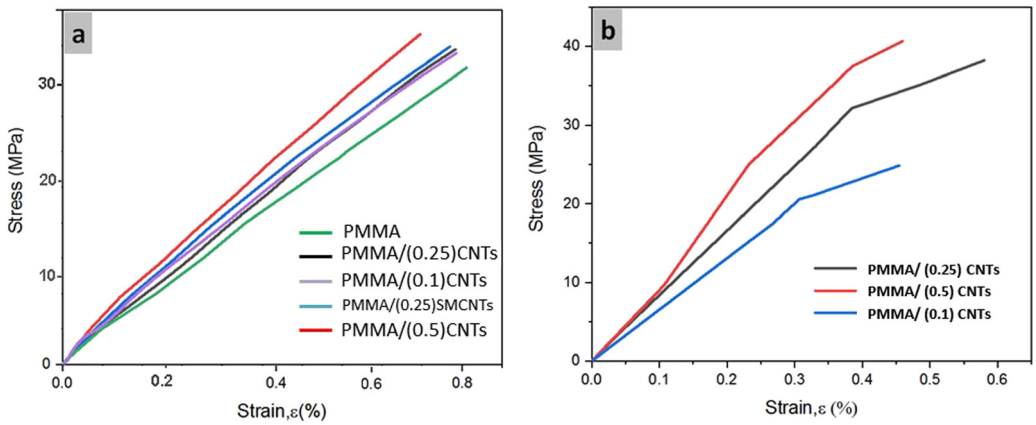

Fig. 9 Stress–strain curves obtained from (a) experimental procedure and (b) numerical estimation.

findings suggest a decrease in the aggregation of CNTs and a reduction in the number of areas in the cement microstructure that had a high concentration of stress. Therefore, more load is needed to generate more strain in nanocomposites. Also, the data obtained from elongation measurements show that there is a slight decrease in the values for PMMA bone cement contained 0.1 and 0.5 wt% MWCNTs. This reduction agrees with TS and EM values and indicates that MWCNTs have strengthened the PMMA matrix suitably.

The effects of surface modification of the carbon nanotubes with acid treatment on mechanical properties for PMMA/(0.25)MWCNT are also presented in Table 3. As seen, surface modification treatment brings the TS and EM to higher values, and the elongation at the break slightly decreases by about 0.1%. It can be attributed to the better adhesion of CNTs to the matrix, which is related to the generated polar functional groups on the surface of MWCNT shells.[27] Indeed, as has been observed by previous studies, such acid treatments can shorten the nanotubes and change their cross sections by occurring local oxidations. As a result, the shorter MWNCTs restrict the application deformation to nearby locations in the PMMA, requiring greater stresses to reach the fracture threshold.[29,30]

Finite element results from estimating the elongation, EM, and TS of three different nanocomposites are also shown in Table 3. The values obtained from FEA solutions have good conformity with the experimental results, with an error variance of less than 20%. Fig. 8 shows how the three main mechanical properties vary with the weight percent of MWCNTs and compare numerical and experimental measurements.

The stress–strain curves for experimental and finite element methods are shown in Fig. 9. As demonstrated in Fig. 9a, experimental specimens of PMMA and nanocomposites have elastic behavior, which agreed with previous studies.[32,34] It can be found that when the amount of CNTs has increased, the fracture occurs at lower values of %ε. Also, Fig. 9b shows that the numerical estimation results have the same elastic behavior with an error of less than 20%. In both figures, with the addition of CNTs up to 0.5 wt%, for the same reasons mentioned above, the composites became strengthened gradually.

The graphical Von-Mises stress distribution is represented in Fig. 10. It can be found from the graphs that the stress concentration increases around the clustered inclusions in the models with 0.1 and 0.25 wt% CNTs. With the increase of the reinforcement phase in the PMMA matrix, the results agree with those explained above. So it is indicated that PMMA contained 0.5 wt% of CNTs tolerated more stresses than others (see Fig. 9a) without a considerable strain enhancement around

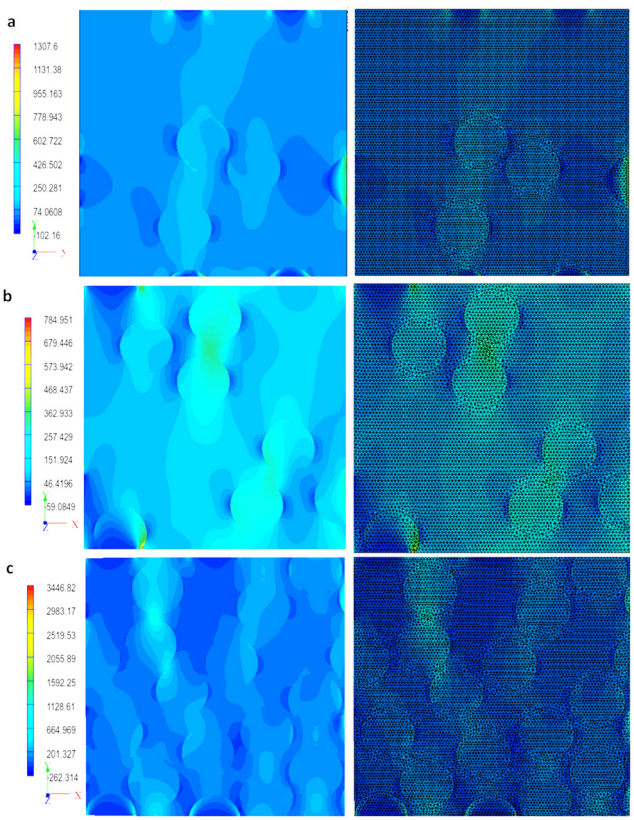

Fig. 10 Graphical Von-Mises stress distribution of the meshed and unmeshed models of (a) PMMA/(0.1)CNTs, (b) PMMA/(0.25)CNTs and (c) PMMA/(0.5)CNTs.

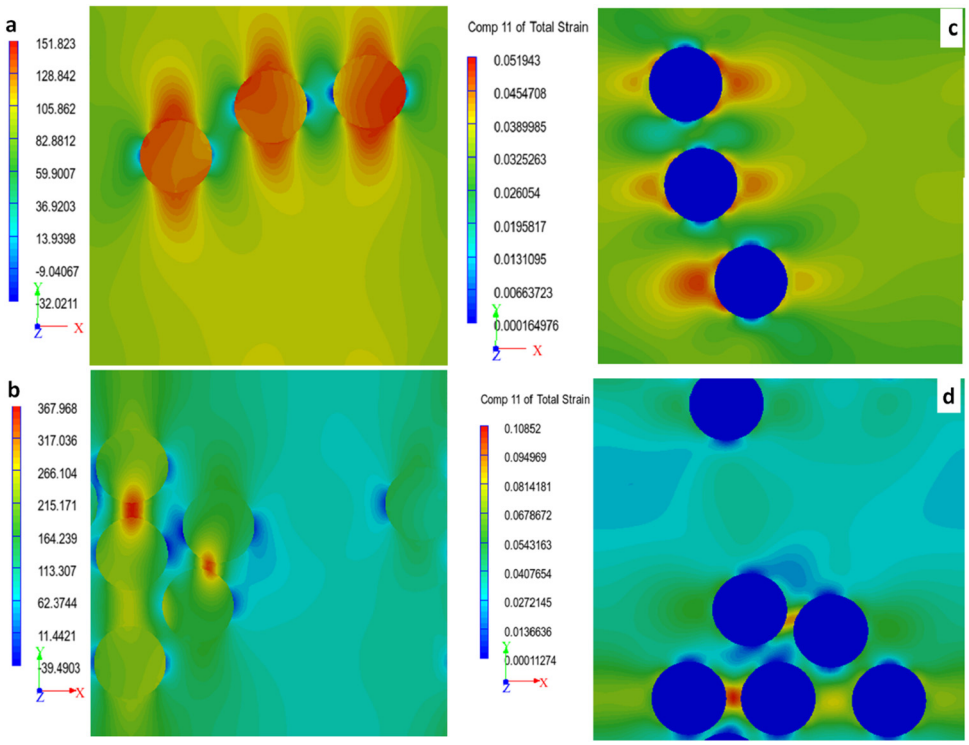

Fig. 11 (a and b) Graphical Von-Mises stress and (c and d) e11 distribution of clustered CNTs in PMMA/(0.1)CNTs, and PMMA/(0.25)CNTs.

the nanotubes. Also, transferring stress to inclusions has occured better in the 0.5 wt% CNT nanocomposites. The maximum tensile strain component, e11, is predicted to be about 0.05 in the lower content and 0.01 in the high content nanocomposites. These results can be confirmed by the other reports of the computational estimations.[31–34] The effect of clustering in the low-content composites was also studied on Von-Mises stress and strain values. The clustering does not affect the numerical solution by using the random algorithm because of the determined space between particles. Fig. 11 shows an increase in stresses and strains between particles as maximum Von-Mises stress reaches 151 and 367 MPa for the PMMA-0.1CNTs and PMMA-0.25CNTs models, respectively. The graphical illustration of e11 is also displayed in Fig. 11 for the clustered type composites. Similar to the stress distribution, the value of e_{11} increases significantly around the agglomerated particles so far that it reaches the maximum amount of 0.05 for both PMMA nanocomposites. Examining the fracture surfaces obtained from the tensile test shows the microstructure and distribution of the CNTs in the sample. Besides, it helps to determine the failure mechanism and, subsequently, the curing mechanism of the polymer matrix in the nanobiocomposite.

SEM images of the fracture surface of the PMMA and nanobiocomposites are shown in three magnifications in Fig. 12. The failure mechanism in the sample of PMMA without CNTs (control sample), is crack growth or agglomeration of the cement powders during the curing procedure or failure occurring in the cavities. In brief, the reinforcement mechanisms of CNTs in the PMMA-MWCNT nanobiocomposites include bridging of CNTs between the initiated crack in the matrix, which leads to preventing the crack growth, crack deflection in the presence of CNTs during crack growth, pulling out of CNTs that reduces the degree of applied force.[32,33] In FESEM images, it is seen that CNTs have been pulled out (shown in the figures with yellow arrows) from the polymer matrix. This phenomenon occurs because the surface shear strength between CNTs and the PMMA matrix is smaller than the tensile strength of MWCNTs, which is around 2 TPa. Fig. 12c and e exhibit the fracture surfaces of nanobiocomposites containing MWCNTs with and without surface modification. It is observable that the pull-out of MWCNTs in PMMA/(0.25)CNTs is more than PMMA/(0.25)SMCNTs, which indicates the better adhesion of surface-modified CNTs to the polymeric phase. Their interface did not split under tension; however, when employing complete MWCNTs, the contact between the nanotubes and polymer matrix decreased due to chemical bonding weakness.[27–30]

3.2 Crack bridging modeling by the finite element method

Crack bridging is one of the important mechanisms for strengthening polymer/CNT nanocomposites, and it has been reported in other research reports. Nevertheless, the numerical prediction of how this mechanism affects the reinforcing mode is still in the initial state. This study employed the finite element method (FEM) for simulating the bridging mechanism PMMA/multi-walled carbon nanotube nanocomposite. A nanocomposite model of the randomly-distributed aligned CNTs was designed in the first step (Fig. 13a), and then a simple vertical notch was defined in this structure. For comparison,

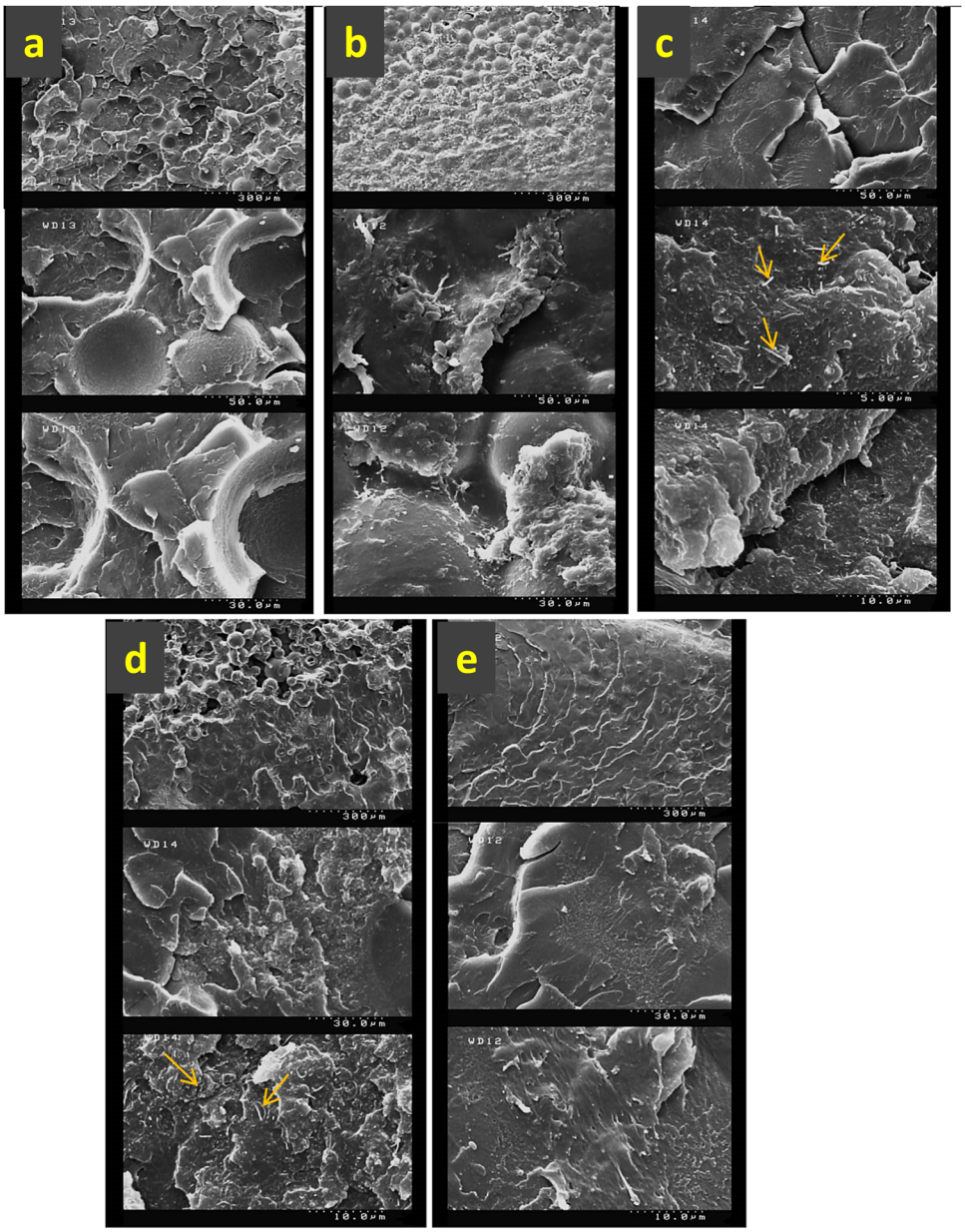

Fig. 12 FESEM images from fracture surfaces of (a) PMMA, (b) PMMA/(0.1)CNTs, (c) PMMA/(0.25)CNTs, (d) PMMA/(0.5)CNTs and (e) PMMA/(0.25)SMCNT which are obtained from tensile test.

this structure was built without a carbon nanotube as a control model. Von-mises stress distribution in the matrix, around the carbon nanotubes and crack, was calculated. The calculated Mises stress showed that the maximum stress zones are concentrated around the carbon nanotubes and crack tip (Fig. 13b and c). The value of stress values in the matrix is small. However, this parameter has the highest value in the center of the nanotubes rather than in other places in the sample (Fig. 13c). These results are attributed to the high elastic modulus values of multi-walled nanotubes, which support the effective role of the load-bearing capacity of these nanofibers in the PMMA matrix. The amounts of stress in the crack's vicinity for polymer nanocomposites were compared with a sample without nanofiber, and the outcomes confirmed that this parameter is two times less for the pristine polymer. These results proved that crack bridging is a dominating mechanism that suppresses crack growth in nanocomposite samples.

3.3 Bending properties

The flexural stress–strain graphs of PMMA nanobiocomposites and graphs which have been obtained from finite element prediction are shown in Fig. 14(a and b). In the experimental results, it can be seen from Fig. 14a that the monolithic PMMA matrix exhibits an elastic response to applied load of up to about 0.02% of bending strain. At the further strains, the matrix shows small nonlinear deformation before reaching

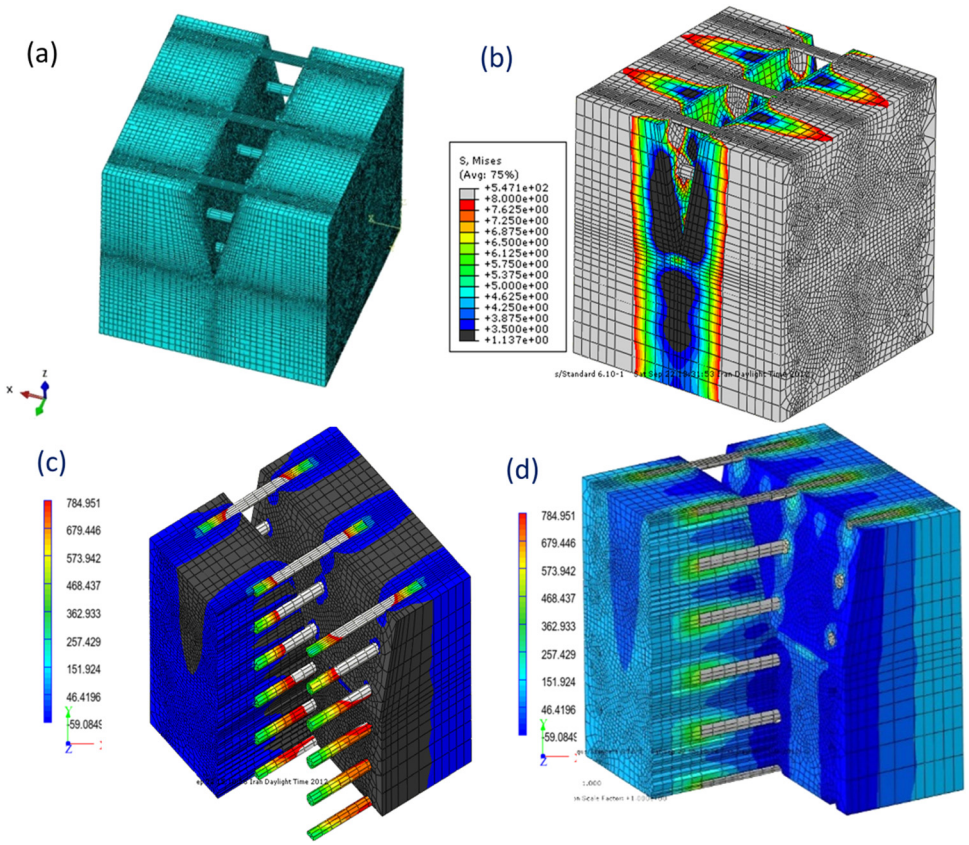

Fig. 13 (a) The used geometry of a PMMA-CNT nanocomposite, and the stress distribution (b) around the crack (c) across the nanotubes.

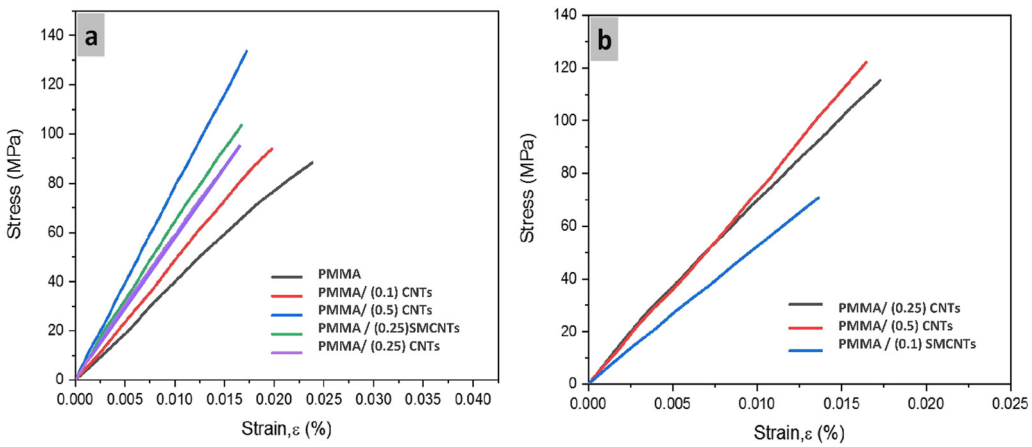

Fig. 14 Flexural stress–strain curves obtained from (a) experimental procedure and (b) numerical estimation.

failure. The results of both experimental and finite element approaches reveal that the nanocomposites exhibit linear behavior and brittleness under the applied load after adding carbon nanotubes to the initial phase. The diagrams demonstrate that the final elongation before fracture for samples with pristine PMMA is higher than others.

The flexural strength (FS) measurements by the experimental and FEA methods are presented in Fig. 15b. Experimental outcomes exhibit that the flexural strength results gained from nanocomposite have higher amounts by adding nanotubes in comparison with the control sample (PMMA). For instance, with 0.1 and 0.5 wt% of MWCNTs, the FS values increased by 20% and 56%, respectively. This comparative chart also investigates the influence of acid treatment on flexural strength. As it is represented, surface modification of nanotubes causes an improvement in FS by 10%. Moreover, the finite element estimation of FS for different samples shows that the values are in agreement with experimental data with an error percent of less than 15%.

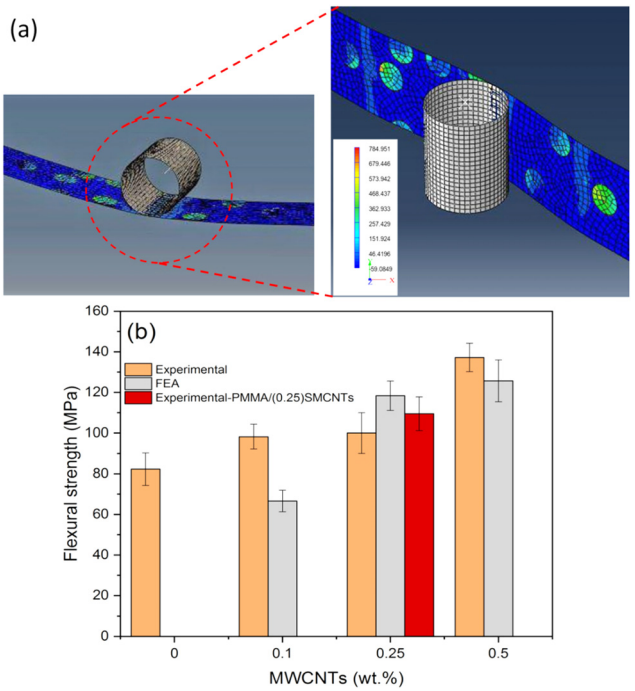

Fig. 15 (a) The Von-Mises stress distribution during the FEA modeling of PMMA-MWCNTs under bending load, and (b) comparative bar chart of flexural strength of PMMA-based bone cement with 0, 0.1, 0.25 and 0.5 wt% of MWCNTs.

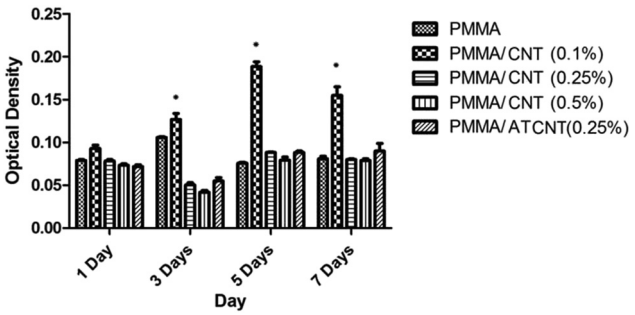

Fig. 16 Comparative bar chart of optical density of mesenchymal stem cells for 0, 0.1, 0.25, and 0.5 wt% of CNTs. Note: ATCNT= acid treated CNT.

The stress distribution graph from the simulation process of a three-point bending test and the stress shielding effect of CNTs can be observed in Fig. 15a. A lower stress level is represented by dark blue in the PMMA matrix, and higher bending stress levels are displayed by bright blue to green and orange in some regions around CNTs. It should be noted that the moving punch was defined as a rigid body; therefore, there is no change in stress level, as shown in the graph.[30–32]

3.4 Biocompatibility assay results

The MTT test was used to investigate the biocompatibility and the effect of CNTs on the growth and proliferation of mesenchymal stem cells. The results of the growth and proliferation assays of the nanobiocomposites and the control sample are given in Fig. 16 as an average of three repetitions for 1, 3, 5, and 7 days. The addition of MWCNTs to the PMMA matrix did not produce cytotoxicity and did not create a negative response by contact with mesenchymal stem cells. As shown in the figure, the maximum cell growth is related to nanobiocomposite containing 0.1 wt% MWCNTs due to the low amount of the nanotubes and optimum topography of the nanobiocomposite surface. The cell viability of other samples is almost at the same level. The fluorescence microscopy images of the grown cells on the samples after 7 days are shown in Fig. 17. The bright spots in the images prove the number of living cells after 7 days near the PMMA and nanobiocomposites. As seen, the results given in Fig. 15 correspond to those in Fig. 16, and the maximum living cells are visible adjacent to the PMMA nanobiocomposite containing 0.1 wt% MWCNTs.

PMMA is a well known bone cement biomaterial and the Food and Drug Administration has approved it for medical application since 2002. However, this polymer has some drawbacks, including the exothermic reaction during its polymerization process. PMMA polymerization is a highly exothermic reaction therefore it may cause the death of the bone tissue or thermal necrosis. As a result of this reaction heat of about 1.4–1.7 $\times$ 108 J per cubic meter of the cement is generated and consequently the temperature can reach 70–120 °C. There are several studies[35] that prove that the incorporation of MWCNTs in PMMA results in dissipation of the heat generated during the reaction by improving the conductivity of bone cement and acting as a heat sink. Moreover, during the polymerization reaction physical and chemical interaction between MWCNT network in the PMMA microstructure are formed. These phenomena can result in the reduction of heat energy generated during polymerization reaction. These mechanisms results in decreasing maximum temperature reached during the curing process and also increase the setting time by incorporation of MWCNTs into PMMA.[36] Furthermore, lower thermal necrosis of the surrounding tissue will be generated. Moreover, a decrease in exothermic polymerization reaction of PMMA based bone cement reduce residual stresses and as a result possibility of premature failure of the cement mantle decreases. Biocompatibility has two aspects: one aspect is its "*in vitro*" biocompatibility and another side is "*In vivo*" biocompatibility of biomaterials. This paper investigated the invitro biocompatibility of synthesized PMMA-CNT bone cement outside the body and the results showed that this type of biocompatibility will increase by adding 0.1 wt% CNT nanotubes. In addition, it can be assumed that adding nanotube will decrease its exothermic reaction temperature. However, the concern about application PMMA is serious and many researchers around the world are working to solve curing temperature drawback.

4 Conclusion

In the current research work, we tried to investigate the enhancement of mechanical properties of PMMA-based bone cement by making nanocomposites with different weight percents

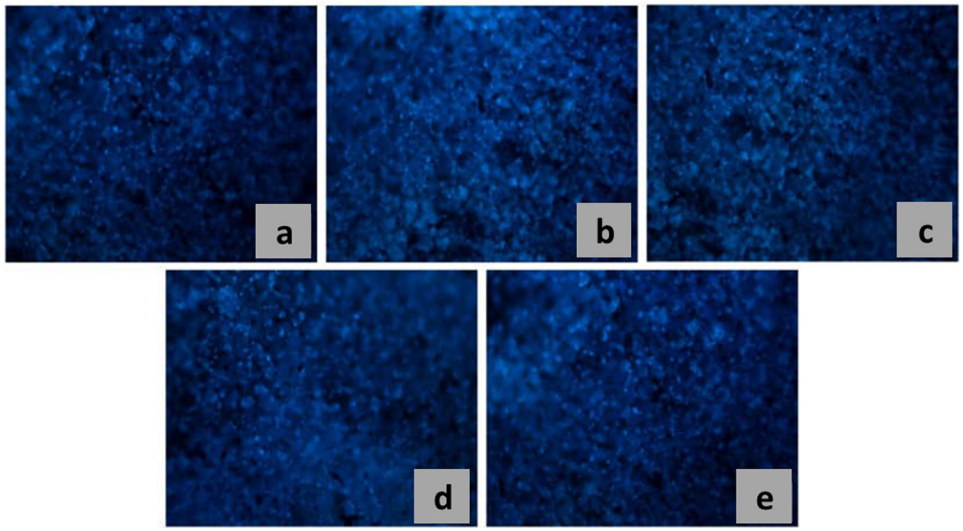

Fig. 17 Fluorescent microscopy images from proliferation of mesenchymal stem cells after 7 days on (a) PMMA, (b) PMMA/(0.1)CNTs, (c) PMMA/(0.25)CNTs, (d) PMMA/(0.5)CNTs and (e) PMMA/(0.25)SMCNT.

of MWCNTs. In this regard, the two experimental and numerical methods were employed to examine the mechanical properties of PMMA-MWCNT nanocomposites. We applied the casting method to synthesize the composite samples with the content of 0.1, 0.25, and 0.5 wt% MWCNTs. The effects of increasing CNT contents on the mechanical properties of the cement were assessed by the conventional tests. To perform the numerical calculations, we used a two-dimensional representative volume element (RVE) generated by the new software, Digimat-EXstream. Results show an overall enhancement in the properties by increasing the content of the nanotubes in the composites. For instance, the average elastic modulus value increased from 2413 MPa for pristine-PMMA to 3369 MPa for PMMA-(0.5) CNT sample.

The effect of the acid treatment on mechanical properties was also investigated. According to the results, by surface modification of MWCNTs, elastic modulus and tensile strength grew by 20% and 2%, respectively. The finite element results of four main mechanical properties represent a good correlation between experimental and numerical data with an error of less than 20%. This study also confirmed that the clustering of the nanotubes in the polymer matrix could weaken the reinforcing effect. The flexural stress results show that by increasing the CNT in the nanocomposites, considerable growth in this property can be achieved. The finite element method was utilized to simulate the crack-bridging mechanism, which is the most essential strengthening mechanism. MTT results reveal that increasing the concentration of CNTs in the PMMA nanocomposites allows mesenchymal cells to survive and proliferate enough on the nanocomposites. However, there is an optimal CNT content for the viability of cells. As the amount of CNTs increases over 0.25 wt%, the cell density drops considerably.

Conflicts of interest

There are no conflicts to declare.

Acknowledgements

The technical supports of this study from the University of Tehran and Sharif University of Technology are gratefully acknowledged. Also, the authors would like to acknowledge valuable assistance from the Institutes for NanoBiomedical Research, Rutgers University. We are especially grateful to anonymous reviewers for their valuable and constructive comments.

References

1 J. N. Coleman, U. Khan, W. J. Blau and Y. K. Gun'ko, Small but strong: a review of the mechanical properties of carbon nanotube–polymer composites, *Carbon*, 2006, **44**(9), 1624–1652.
2 E. T. Thostenson, Z. Ren and T.-W. Chou, Advances in the science and technology of carbon nanotubes and their composites: a review, *Composites Sci. Technol.*, 2001, **61**(13), 1899–1912.
3 G. Mittal, V. Dhand, K. Y. Rhee, S.-J. Park and W. R. Lee, A review on carbon nanotubes and graphene as fillers in reinforced polymer nanocomposites, *J. Ind. Eng. Chem.*, 2015, **21**, 11–25.
4 R. E. Shalin, *Polymer Matrix Composites*, first edn, 1996.
5 J. Łukaszczyk, M. Śmiga-Matuszowicz, K. Jaszcz and M. Kaczmarek, Characterization of new biodegradable bone cement compositions based on functional polysuccinates and methacrylic anhydride, *J. Biomater. Sci.: Polym. Edn*, 2007, **18**(7), 825–842.
6 A. Kamyar, M. Khakbiz, A. Zamanian and M. Yasaei, BenyaminYarmand, Synthesis of a novel dexamethasone intercalated layered double hydroxide nanohybrids and their deposition on anodized titanium nanotubes for drug delivery purposes, *J. Solid State Chem.*, 2019, **271**(6), 144–153.

7 V. N. Popov, Carbon nanotubes: properties and application, *Mater. Sci. Eng., R*, 2004, **43**(3), 61–102.
8 Y.-H. Nien, *The Application of Carbon Nanotube to Bone Cement. In Carbon Nanotubes-Polymer Nanocomposites*. IntechOpen, 2011.
9 R. Ormsby, T. McNally, P. O'Hare, G. Burke, C. Mitchell and N. Dunne, Fatigue and biocompatibility properties of a poly (methyl methacrylate) bone cement with multi-walled carbon nanotubes, *Acta Biomater.*, 2012, **8**(3), 1201–1212.
10 Y.-H. Nien and C.-l Huang, The mechanical study of acrylic bone cement reinforced with carbon nanotube, *Mater. Sci. Eng., B*, 2010, **169**(1-3), 134–137.
11 R. Ormsby, T. McNally, C. Mitchell and N. Dunne, Influence of multi-wall carbon nanotube functionality and loading on mechanical properties of PMMA/MWCNT bone cements, *J. Mater. Sci.: Mater. Med.*, 2010, **21**, 2287–2292.
12 B. G. Demczyk, Y. M. Wang, J. Cumings, M. Hetman, W. Han, A. Zettl and R. O. Ritchie, Direct mechanical measurement of the tensile strength and elastic modulus of multi-walled carbon nanotubes., *Mater. Sci. Eng., A*, 2002, **334**(1-2), 173–178.
13 R. George, K. T. Kashyap, R. Rahul and S. Yamdagni, Strengthening in carbon nanotube/aluminium (CNT/Al) composites., *Scr. Mater.*, 2005, **53**(10), 1159–1163.
14 D. Qian, E. Co Dickey, R. Andrews and T. Rantell, Load transfer and deformation mechanisms in carbon nanotube-polystyrene composites, *Appl. Phys. Lett.*, 2000, **76**(20), 2868–2870.
15 B. Jiang, C. Liu, C. Zhang, B. Wang and Z. Wang, The effect of non-symmetric distribution of fiber orientation and aspect ratio on elastic properties of composites, *Composites, Part B*, 2007, **38**(1), 24–34.
16 E. T. Thostenson and T.-W. Chou, Aligned multi-walled carbon nanotube-reinforced composites: processing and mechanical characterization, *J. Phys. D: Appl. Phys.*, 2002, **35**(16), L77.
17 J. M. Wernik and S. A. Meguid, Multiscale modeling of the nonlinear response of nano-reinforced polymers., *Acta Mech.*, 2011, **217**(1–2), 1–16.
18 B. R. Reddy and K. Ramji, Modeling and Simulation of Nano and Multiscale Composites, *Int. J. Hybrid Inf. Technol.*, 2016, **9**(3), 133–144.
19 R. Rafiee and R. M. Moghadam, Simulation of impact and post-impact behavior of carbon nanotube reinforced polymer using multi-scale finite element modeling., *Comput. Mater. Sci.*, 2012, **63**, 261–268.
20 N. K. C. Tummalapalli. *Experimental Characterization and Simulation of Carbon Nanotube Strain Sensing Films.* (2016).
21 B. Zhang, Z. Yang, X. Sun and Z. Tang, A virtual experimental approach to estimate composite mechanical properties: modeling with an explicit finite element method., *Comput. Mater. Sci.*, 2010, **49**(3), 645–651.
22 H. W. Wang, H. W. Zhou, L. Mishnaevsky Jr, P. Brøndsted and L. N. Wang, Single fibre and multifibre unit cell analysis of strength and cracking of unidirectional composites, *Comput. Mater. Sci.*, 2009, **46**(4), 810–820.
23 H. W. Wang, H. W. Zhou, R. D. Peng and L. Mishnaevsky Jr., Nanoreinforced polymer composites: 3D FEM modeling with effective interface concept, *Composites Sci. Technol.*, 2011, **71**(7), 980–988.
24 I. Gitman, H. Askes and L. Sluys, Representative volume: existence and size determination, *Eng. Fract. Mech.*, 2007, **74**(16), 2518–2534.
25 Y. Liu and X. Chen, Evaluations of the effective material properties of carbon nanotube-based composites using a nanoscale representative volume element, *Mech. Mater.*, 2003, **35**(1–2), 69–81.
26 C. Zeng, N. Hossieny, C. Zhang, B. Wang and S. M. Walsh, Morphology and tensile properties of PMMA carbon nanotubes nanocomposites and nanocomposites foams, *Compos. Sci. Technol.*, 2013, **82**, 29–37.
27 S. Saha and S. Pal, Mechanical properties of bone cement: a review, *J. Biomed. Mater. Res.*, 1984, **18**(4), 435–462.
28 G. Lewis, Properties of acrylic bone cement: state of the art review, *J. Biomed. Mater. Res.*, 1997, **38**(2), 155–182.
29 P. Guo, X. Chen, X. Gao, H. Song and H. Shen, Fabrication and mechanical properties of well-dispersed multi-walled carbon nanotubes/epoxy composites., *Composites Sci. Technol.*, 2007, **67**(15–16), 3331–3337.
30 D. Blond, V. Barron, M. Ruether, K. P. Ryan, V. Nicolosi, W. J. Blau and J. N. Coleman, Enhancement of modulus, strength, and toughness in poly(methyl methacrylate)-based composites by the incorporation of poly(methyl methacrylate)-functionalized nanotubes., *Adv. Funct. Mater.*, 2006, **16**(12), 1608–1614.
31 R. D. Peng, H. W. Zhou and H. W. Wang, and Leon Mishnaevsky Jr. Modeling of nano-reinforced polymer composites: Microstructure effect on Young's modulus, *Comput. Mater. Sci.*, 2012, **60**, 19–31.
32 I. Viejo, L. P. Esteves, M. Laspalas and J. M. Bielsa, Numerical modelling of porous cement-based materials by superabsorbent polymers., *Cem. Concr. Res.*, 2016, **90**, 184–193.
33 X. Yue and E. Weinan, The local microscale problem in the multiscale modeling of strongly heterogeneous media: Effects of boundary conditions and cell size, *J. Comput. Phys.*, 2007, **222**(2), 556–572.
34 H. Qing, Automatic generation of 2D micromechanical finite element model of silicon–carbide/aluminum metal matrix composites: Effects of the boundary conditions., *Mater. Des.*, 2013, **44**, 446–453.
35 R. Ormsby, T. McNally, C. Mitchell, P. Halley, D. Martin, T. Nicholson and N. Dunne, Effect of MWCNT addition on the thermal and rheological properties of polymethyl methacrylate bone cement, *Carbon*, 2011, **49**(9), 2893–2904.
36 M. Salami-Kalajahi, V. Haddadi-Asl, F. Behboodi-Sadabad, S. Rahimi-Razin and H. Roghani-Mamaqani, Properties of PMMA/carbon nanotubes nanocomposites prepared by "grafting through" method, *Polym. Compos.*, 2012, **33**(2), 215–224.
37 M. Yasaei, M. Khakbiz, A. Zamanian and E. Ghasemi, Synthesis and characterization of Zn/Al-LDH@SiO2 nanohybrid: Intercalation and release behavior of vitamin C, *Mater. Sci. Eng.*, 2019, **103**, 109–124.